Multi-Level Equilibrium Signaling for Molecular Communication

Bayram Cevdet Akdeniz, Malcolm Egan

Multi-Level Equilibrium Signaling for Molecular Communication

Bayram Cevdet Akdeniz and Malcolm Egan
Univ. Lyon, INSA Lyon, INRIA, CITI
Villeurbanne, France

ABSTRACT

Two key challenges in diffusion-based molecular communication are low data rates and accounting for the geometry of the fluid medium in the form of obstacles and the boundary. To reduce the need for the receiver to have knowledge of the geometry of the medium, binary equilibrium signaling has recently been proposed for molecular communication with a passive receiver in bounded channels. In this approach, reversible chemical reactions are introduced at the transmitter and the receiver in order for the system to converge to a known equilibrium state. This provides a means of designing simple detection rules that only depend on the transmitted signal and the volume of the bounded fluid medium. In this paper, we introduce multi-level equilibrium signaling, which allows for higher data rates via higher order modulation. We show that for a wide range of conditions, with appropriate receiver optimization, multi-level equilibrium signaling can outperform conventional concentration shift keying schemes. As such, our approach provides a basis to improve data rates in molecular communications without the need to increase the complexity of the system by exploiting techniques such as multiple information-carrying molecules.

KEYWORDS

Molecular communication, equilibrium signaling, multi level signaling

1 INTRODUCTION

A challenge in diffusion-based molecular communications is low data rate transmission. This challenge arises from two factors: (i) the long time scales involved in molecular diffusion; and (ii) noise in the observed number of molecules at the receiver. The impact of the noise is that modulation schemes of low order––typically, binary––have traditionally been required. Due to the time scale for molecules to diffuse to the receiver, it can take a long time for a single bit to be communicated.

A second challenge is the need for receivers to be adapted to the geometry of the communication channel. For example, conventional concentration shift keying (CSK) schemes require knowledge of the statistics for the quantity of molecules that arrive at the sampling time [12]. However, in practice, it is challenging to estimate the distance between the transmitter and the receiver [5], and even more difficult to characterise the boundary of a complicated biochemical system in which the communication system is embedded. The same issue also arises in other schemes such as molecular shift keying (MoSK) [3] and pulse position modulation schemes [2].

To address the challenge of complex channel geometry, a new binary modulation scheme called equilibrium signaling with a passive receiver has been introduced in [1] for a bounded fluid medium. To the best of the authors' knowledge, equilibrium signaling is the first scheme for molecular communication utilizing a passive receiver allowing for a bounded channel and no degradation of information carrying molecules in the channel. As passive receivers typically require advanced spectroscopy methods, this setup is relevant for microfluidic circuits in the context of lab-on-a-chip systems.

The main innovation in equilibrium signaling is to introduce reversible chemical reactions in the transmitter and the receiver. By doing so, the system converges to an equilibrium state with known Gaussian statistics, dependent only on the number of transmitted molecules and the volume of the system. As such, a passive receiver does not require knowledge of the shape of the boundary or obstacles within the system.

While equilibrium signaling forms a basis to address the second challenge, it is necessary for the receiver to sample near the equilibrium state which only exacerbates the challenge of low data rates. While low data rates may be unavoidable in systems exploiting biological circuits [1], it is not desirable in general; particularly in the context of microfluidic circuits where advanced spectroscopy methods may be available.

In this paper, we propose a method in order to increase the data rate for molecular communications based on equilibrium signaling. To do so, we introduce multi-level equilibrium signaling, where the transmitter can exploit a higher-order modulation scheme allowing for $M > 2$ symbols. Multi-level equilibrium signaling exploits the possibility, as a passive receiver is utilised, of obtaining multiple independent observations for each transmitted symbol. The consequence is that the strength of the noise can be dramatically reduced.

In order to design parameters, we derive an accurate approximation for the probability of error for multi-level equilibrium signaling. This provides a basis to optimise the order of the modulation scheme and to choose appropriate amplitudes subject to constraints on the number of samples available at the receiver.

Due to the difficulty in reducing the strength of the noise at the receiver, conventional approaches such as CSK have typically exploited binary modulation schemes and been limited to systems either with an absorbing receiver, channels with unbounded volume or information molecule degradation. Higher order modulation schemes based on MoSK have also been proposed at the cost of a large number of types of information-carrying molecules. To establish the performance of multi-level equilibrium signaling, we compare it with CSK and show significant performance improvements in terms of the probability of error.

2 SYSTEM MODEL

Let $\Omega \subset \mathbb{R}^d$, $d \in \{1, 2, 3\}$ be a domain with smooth boundary $\partial\Omega$ consisting of transmitting and receiving devices with a fluid medium separating the devices. Consider the discretization of Ω

into N volume elements (voxels) each of volume V_{vox}, with the set of points in voxel i denoted by $\mathcal{V}_i,\ i = 1, \ldots, N$. Here, volume is interpreted as length in $\mathbb{R}^1$, area in $\mathbb{R}^2$, and volume in $\mathbb{R}^3$. The setup for a one-dimensional channel is illustrated in Fig. 1, where the receiver may lie in the interior of the bounded channel.

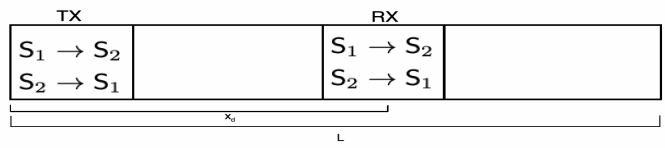

Figure 1: System Model.

Messages to be sent by the transmitter with volume V_{Tx} are encoded into the quantity of the chemical species S_1. Within the transmitter and the receiver, each species is produced or removed via the unimolecular reactions

$$\begin{aligned} \mathrm{S}_1 &\to \mathrm{S}_2 \\ \mathrm{S}_2 &\to \mathrm{S}_1, \end{aligned} \tag{1}$$

In particular, the transmitter produces information-carrying molecules of species S_2 by the first reaction in (1). In general, a more complex reaction pathway may be present; however, the intermediate reactions occur rapidly as is common, for example, in enzyme-based reactions.

We assume that molecules of species S_1 produced in the transmitter are not capable of diffusing into the channel. On the other hand, this is possible for species S_2.

In order to capture the effect of small quantities of each chemical species in the system (i.e., $\mathrm{S}_1, \mathrm{S}_2$), we consider a stochastic model for the kinetics. To formally describe the scenario, we introduce the following notation. Let $M_i^l(t),\ l = 1, 2,\ i = 1, \ldots, N$ denote the random variable for the number of molecules of species S_1 or S_2 in voxel i at time t. Denote $\mathbf{M}_i(t) = [M_i^1(t), M_i^2(t)]$ as the state vector in voxel i and the matrix $\mathbf{M}(t) = [\mathbf{M}_1(t), \ldots, \mathbf{M}_N(t)]$. The probability that $\mathbf{M}(t)$ has value $\mathbf{m}$ at time t is then denoted by

$$P(\mathbf{m}, t) = \Pr(\mathbf{M}(t) = \mathbf{m} | \mathbf{M}(0) = \mathbf{m}_0), \tag{2}$$

where $\mathbf{M}(0)$ is the initial quantity of molecules of each species in each voxel. In the present context, the $\mathbf{M}(0)$ is dependent on the equilibrium state of the biochemical process under observation.

Since each reaction is unimolecular, it follows that in each reaction the number of molecules of the two species involved can only increase or decrease by one. Let 1_i^l be the state where the number of molecules in all voxels is zero, except for species l in voxel i. That is, $\mathbf{M}(t) + 1_i^l$ means that the number of molecules of species l in voxel i is increased by one.

A popular model for stochastic kinetics of molecules is the reaction-diffusion master equation (RDME) [11], also utilized in the context of molecular communications in [6]. In this model, the diffusive jump rate is denoted by κ_{ij}^l for each individual molecules of the l-th species moving from voxel j into voxel i, with $\kappa_{ii} = 0,\ i = 1, \ldots, N$. In particular, the probability per unit time that a molecule of S_l diffuses from voxel j to voxel i at time t is given by $\kappa_{ij}^l M_j^l(t)$. We expect that in many microfluidic systems, κ_{ij}^l is constant for a given species S_l over all voxels i, j. Nevertheless, it is also possible to consider spatially inhomogeneous diffusion [1].

In the case of mass-action kinetics and first-order reactions, the probability per unit time that a molecule of S_l in voxel i reacts at time t is given by $a_i^l M_i^l(t)$ with rate constants a_i^l. In general, the reaction rate is dependent on the voxel index. The net change of each chemical species due to the reaction with substrate S_l is expressed via the column vector $\boldsymbol{\nu}_l \in \mathbb{N}^2$. The term $\boldsymbol{\nu}_l 1_i$ indicates that $\mathbf{M}(t)$ changes by $\boldsymbol{\nu}_k$ in the i-th voxel.

In order to model production of S_1 in the transmitter and S_2, we assume that for voxels i comprising the transmitter and the receiver $a_i^l = a^l$, while $a_i^1 = 0$ for voxels comprising the channel.

In the RMDE model, the probability distribution $P(\mathbf{m}, t)$ evolves according to the system of differential equations given by

$$\begin{aligned} &\frac{\mathrm{d}P(\mathbf{m}, t)}{\mathrm{d}t} \\ &= \sum_{i=1}^{N} \sum_{j=1}^{N} \sum_{l=1}^{2} \Big(\kappa_{ij}^l (m_j^l + 1) P(\mathbf{m} + 1_j^l - 1_i^l, t) \\ &\quad - \kappa_{ji}^l m_i^l P(\mathbf{m}, t) \Big) + \sum_{i=1}^{N} \sum_{l=1}^{2} \Big(a_i^l (m_i^l + 1) P(\mathbf{m} - \boldsymbol{\nu}_l 1_i, t) \\ &\quad - a_i^l m_i^l P(\mathbf{m}, t) \Big). \end{aligned} \tag{3}$$

The system of ordinary differential equations in (3) corresponds to the Kolmogorov forward equation for a continuous-time Markov chain; that is, the evolution of the system state is Markovian. In our setting, the Markov chain corresponding to the RDME is irreducible and positive recurrent. Therefore, a stationary distribution exists and is given by [9]

$$\pi(\mathbf{m}) = \lim_{t \to \infty} \Pr(\mathbf{M}(t) = \mathbf{m} | \mathbf{M}(0) = \mathbf{m}_0). \tag{4}$$

3 MULTI-LEVEL EQUILIBRIUM SIGNALING

3.1 Signaling

We assume that the system operates using time slots with duration T_s and that no molecules of species S_1 nor S_2 are present in the system at $t = 0$. The symbol to be transmitted in time slot n is denoted by $s_n \in \{1, \ldots, M\}$. Moreover, molecules that are produced by the transmitter may change the number of each species via the reactions in (1); however, no molecules degrade.

Consider the n-th time slot. Due to the previous $n-1$ transmissions, there are $N_{\text{Tx},l}(nT_s),\ l = 1, 2$ molecules of species S_l in the transmitter. At a time $nT_s + \delta$ shortly after the beginning of the time slot, the biochemical process produces Δ_n^i of S_1 to convey the i-th symbol where $i \in \{1, \ldots, M\}$. In particular, when symbol i is transmitted,

$$N_{\text{Tx},1}(nT_s + \delta) = N_{\text{Tx},1}(nT_s) + \Delta_n^i \tag{5}$$

for $\delta > 0$ a sufficiently small period of time; that is, δ is chosen such that no reactions occur nor any molecules diffuse into the microchannel. We assume that for each time slot, the same quantity of molecules is used to represent a given symbol; i.e., $\Delta_1^i = \Delta_n^i = \Delta^i$.

The key idea behind the proposed multi-level equilibrium signaling strategy is that for sufficiently large T_s, the total number of molecules of species S_1 and S_2 in the detection chamber at the

time of sampling will be approximately drawn from the stationary distribution of the RDME. As such, if the stationary distribution is known, then near-optimal detection rules can be obtained. Furthermore, this property provides a means of using multiple observations to reduce the variance of the observed signal.

3.2 Statistics for the Quantity of S_1

To obtain the statistics for the quantity of S_1 in the receiver—i.e., $N_{\text{Rx},1}(nT_s),\ n = 1, 2, \ldots$—we first consider the case $n = 1$. Suppose that a symbol s_1 is to be transmitted. Then, the following assertion provides an accurate approximate characterization of $N_{\text{Rx},1}(T_s)$, for sufficiently large T_s.

Assertion 1. *Let $N_{\text{Rx},1}(T_s|s_1)$ denote the number of molecules of S_1 in the receiver at time T_s given a transmission of message s_1 corresponding to an emission of Δ_1^i molecules of S_1 for transmitting symbol i. Then,*

$$N_{\text{Rx},1}(T_s|s_1 = i) \sim \mathcal{N}(\mu_1^i, \mu_1^i), \tag{6}$$

where $\mu_1^i > 0$ is a known constant, only dependent on the volume of the enclosing container and not the specific geometry, and $\mathcal{N}(\mu, \sigma^2)$ denotes the Gaussian law with mean μ and variance σ^2. In particular,

$$\mu_1^i = \frac{a^1}{a^2} \frac{\Delta_1^i \frac{V_{\text{Rx}}}{V_{\text{tot}}}}{1 + \frac{a^1}{a^2} \frac{V_{\text{Tx}}+V_{\text{Rx}}}{V_{\text{tot}}}}, \tag{7}$$

where V_{tot} is the total volume of the system.

Under the assumptions that $a^1 = a^2$ and $V_{\text{Tx}} = V_{\text{Rx}}$

$$\mu_1^i = \frac{\Delta_1^i V_{\text{Rx}}}{V_{\text{tot}} + 2V_{\text{Rx}}}. \tag{8}$$

Assertion 1 has been justified for a single transmission in the binary case in [1] based on both theoretical and empirical evidence. It is straightforward to extend the argument to the case of non-binary modulation.

Suppose now that a sequence of equilibrium states, $S^n = [s_1, \ldots, s_n]$, over a period of n sampling intervals is sent. Let the quantity of S_1 at time nT_s given the sequence of transmissions S^n be denoted by $N_{\text{Rx},1}(nT_s|S^n)$. A consequence of Assertion 1 is that under the additional assumption that the observations are independent,

$$N_{\text{Rx},1}(nT_s|S^n) \sim \mathcal{N}(\mu(S^n), \mu(S^n)), \tag{9}$$

where $\mu(S^n) = \mu(S^{n-1}) + \mu_n^{s_n}$ and $\mu(S^1) = \mu_1^{s_1}$. For samples that are sufficiently separated in time, $N_{\text{Tx},1}(T_s)$ is approximately independent of $N_{\text{Tx},1}(2T_s)$, as discussed further in Sec. 4.3.

Let N_s be the number of independent samples that receiver can observe at the equilibrium induced by the transmission of each symbol. Under the assumption of independent observations, it is possible to reduce the variance by averaging these observations and get the symbol $N_{\text{Rx},1}(n+1)$ via

$$N_{\text{Rx},1}(n+1) = \frac{1}{N_s} \sum_{i=1}^{N_s} N_{\text{Rx},1}(t_i|S^n, s_{n+1}), \tag{10}$$

where $t_i \in \{t_1, t_2, \ldots, t_{N_s} : t_i > nT_s\}$. Then the corresponding distribution of $N_{\text{Rx},1}(n+1)$ can be well approximated by

$$N_{\text{Rx},1}(n+1|S^n, s_{n+1} = i) \sim \mathcal{N}(\mu_{n+1}^i + \mu(S^n), \tfrac{\mu_{n+1}^i + \mu(S^n)}{N_s}). \tag{11}$$

3.3 Near Optimal Detection Scheme

Although the observation process is Markovian, for a sufficiently large time slot T_s, the observations $N_{\text{Rx},1}(1), \ldots, N_{\text{Rx},1}(n+1)$ are approximately independent. Let $\mathbf{N}_{\text{Rx},1}$ denote the vector of observations at the receiver for the quantity of S_1 and $\mathbf{s} \in \{1, 2 \ldots M\}^{n+1}$ denote a potential vector of transmitted bits. Under Assertion 1, the joint likelihood of the observations is given by

$$f_{\mathbf{N}_{\text{Rx},1}|\mathbf{s}}(\mathbf{n}) = \prod_{i=1}^{n+1} \frac{1}{\sqrt{\frac{2}{N_s}\pi\mu(S^i)}} \exp\left(-\frac{(n_i - \mu(S^i))^2}{\frac{2}{N_s}\mu(S^i)}\right), \tag{12}$$

and, assuming the independence of elements of $\mathbf{N}_{\text{Rx},1}$, the optimal detection rule is given by

$$\hat{\mathbf{s}}^* = \arg \max_{\mathbf{s} \in \{0,1,\ldots M-1\}^{n+1}} f_{\mathbf{N}_{\text{Rx},1}|\mathbf{s}}(\mathbf{n}). \tag{13}$$

A brute force search for the estimate $\hat{\mathbf{s}}^*$ in (12) leads to a complexity that grows exponentially in n. Nevertheless, the Viterbi algorithm with appropriate branch weights can be used to solve the optimization problem with complexity of order $O(n)$. Note that while the Viterbi algorithm yields an optimal solution for (13), it is under the assumption that Assertion 1 holds.

We briefly sketch the computations in Algorithm 1, which is a form of the Viterbi algorithm with branch metrics tailored to the problem in (12). For the k-th symbol $s_k \in \{0, 1, \ldots M-1\}$, let $p(n_k|s_k) = \log(f_{N_{\text{Rx},1}(kT_s)|s_k}(n_k))$. In the k-th symbol interval, it is necessary to compute P_{k-1,s_k} terms, which correspond to the probability of the most probable sequence until the $k-1$-th symbol and the k-th symbol is for $s_k \in \{1, \ldots M\}$.

Algorithm 1 Near-Optimal Detection Algorithm

1: **Input:** $s_0, u \in \{1, 2, \ldots M\}$, $p(n_k|s_k)$,
2: for $k = 1$ to $n+1$
3: for $i = 1$ to M
$\log P_{k,i} = \max_u \left(\log P_{k-1,u} + p(n_k|s_i)\right)$.
$s_{k,i} = \arg\max_u \log P_{k,u}$.
4: Find the most probable path:
$v = \arg\max_u P_{n+1,u}$.
5: Backtrack this path to obtain $\hat{\mathbf{s}}^*$.

3.4 Low Memory Detection Scheme

For large n, directly solving the optimization problem in (13) requires the storage all previous observations, which may not be desirable. As such, we also consider an approach that only requires limited memory.

A simple and effective detection scheme is the amplitude-based passive receiver proposed in [7]. For this receiver, detection of binary symbols is achieved by comparing two consecutive observed signals. If the current signal is greater than the previous signal, a bit 1 is detected, otherwise a bit 0.

Inspired by this approach, we have developed a detection scheme based on an optimized threshold derived from the statistics of the

difference of two consecutive observations. To this end, define $R(n+1) = N_{\mathrm{Rx},1}((n+1)T_s) - N_{\mathrm{Rx},1}(nT_s)$ which approximately satisfies

$$R(n+1) \sim N(\mu_{n+1}^{s_{n+1}}, \frac{\mu_{n+1}^{s_{n+1}} + 2\mu(S^n)}{N_s}). \tag{14}$$

Under this approximation, we develop the following low memory detection scheme

$$\hat{s}_{n+1} = \min\{u : \ \tau_{u-1} < R(n+1) < \tau_u, \ u = 1, 2, \ldots, M \ \} \tag{15}$$

where $\tau_0 = 0$ and $\tau_M = \infty$. We remark that this scheme extends the low memory detector developed in [1] for binary equilibrium signaling.

To select the thresholds $\tau_1, \ldots, \tau_{M-1}$, note that the probability of error is given by

$$P_e^{M-Eq} = \frac{1}{M}\sum_{i=1}^{M} \Pr(R(n+1|s_i) < \tau_{i-1} \quad \cup \quad R(n+1|s_i) > \tau_i) \tag{16}$$

For sufficiently large n, observe that $\mu(S^n) + \mu_{n+1}^{s_{n+1}} \approx \mu(S^n)$. That is, the variance of $R(n+1)$ is approximately the same for each symbol $s_{n+1} \in \{1, \ldots, M\}$. Under this approximation and using the assumption $\mu_1^i = \mu_n^i = \mu^i$, the thresholds that minimize the probability of error are $\tau_i = \frac{\mu^i + \mu^{i+1}}{2}$, $i = 1, \ldots, M-1$. The corresponding probability of error is then given by

$$P_e^{M-Eq} \approx \frac{1}{M}\sum_{i=1}^{M}\left(1 - Q\left(\frac{\tau_{i-1} - \mu^i}{\mu_{\text{approx}}}\right)\right) + Q\left(\frac{\tau_i - \mu^i}{\mu_{\text{approx}}}\right), \tag{17}$$

where $\mu_{\text{approx}} = n\mu^M$ and $Q(x) = \frac{1}{\sqrt{2\pi}}\int_x^\infty \exp(-u^2/2)\mathrm{d}u$.

4 MULTI-LEVEL EQUILIBRIUM SIGNALING VS CSK

In this section, we study the performance of multi-level equilibrium signaling and provide a comparison with CSK. Conventional CSK schemes—characterized by a sampling time optimized for the peak arrival time of information-carrying molecules—assuming either an absorbing receiver, a bounded channel, or information molecule degradation. As such, to provide a baseline, we first adapt CSK to our system model to form a baseline. We then establish via simulation that multi-level equilibrium signaling outperforms CSK in a wide range of conditions.

4.1 CSK with a Passive Receiver and Bounded Channel

In conventional binary CSK, it is assumed that the quantity, Δ, of S_1 molecules are transmitted when $s_n = 1$, and no molecules of S_1 are transmitted otherwise. Moreover, no other species of molecules are present in the system, molecules of S_1 can diffuse freely, and the quantity of S_1 in the receiver forms the basis for detection. Consider the scenario that the channel is one-dimensional and bounded with length L, and a passive receiver is centered at a position $0 \leq x_d \leq L$. The expected concentration of molecules at the receiver is given by [10]

$$c(x_d, t) = \frac{2\Delta}{\sqrt{4\pi D t}}\sum_{m=-\infty}^{m=+\infty}\left[\exp\left(\frac{-(x_d - 2mL)^2}{4Dt}\right)\right]. \tag{18}$$

Detection in conventional binary CSK is often based on the peak concentration of the underlying deterministic model of diffusion [13]. That is, the sampling time, t_{opt}^{CSK} is chosen such that $c(x_d, t)$ is maximized; i.e.,

$$t_{opt}^{CSK} = arg\max_{t \geq 0} c(x_d, t). \tag{19}$$

As noted earlier, a detection scheme for binary CSK in the presence of a passive receiver, bounded channel, and no information-carrrying molecule degradation has not been developed. To design a detection scheme, we first require the statistics for the quantity of molecules within the receiver at times nt_{opt}^{CSK}, $n = 1, 2, \ldots$, accounting for inter-symbol interference.

Let $M_p = V_{\mathrm{Rx}} c(x_d, t_{opt}^{CSK})$ be the mean number of molecules of S_1 at the receiver at time t_{opt}^{CSK}. Recall that the distribution of molecules of S_1 after the first transmission can be well approximated by $N_{\mathrm{Rx},1}(t_{opt}^{CSK}) \sim \mathrm{Poiss}(M_p)$ (see, e.g., [4]).

In the case that multiple previous transmissions have occurred, we develop an approximation for the statistics of $N_{\mathrm{Rx},1}(nt_{opt}^{CSK})$ with $n > 1$. We first note that for sufficiently large t, the mean quantity of molecules in the system is spatially homogeneous. As such, the mean number of molecules of S_1 in the receiver from each previous transmission of a non-zero quantity of molecules may be approximated by

$$M_e = \frac{\Delta V_{\mathrm{Rx}}}{N V_{\mathrm{Vox}}}. \tag{20}$$

Given a m transmissions of a bit 1, the mean number of molecules of S_1 is then $mM_e + M_p$. As such, for a sufficiently large number of molecules in the channel, we obtain the approximation

$$N_{\mathrm{Rx},CSK}((n+1)T_s | S_n^m, s_{n+1}) \sim \begin{cases} \mathcal{N}(mM_e, mM_e) & s_{n+1} = 0, \\ \mathcal{N}(M_p + mM_e, M_p + mM_e) & s_{n+1} = 1. \end{cases} \tag{21}$$

A natural receiver for binary CSK in our setting then exploits the statistic

$$R(n+1) = N_{\mathrm{Rx},1}((n+1)t_{opt}^{CSK}) - N_{\mathrm{Rx},1}(nt_{opt}^{CSK}). \tag{22}$$

We note that a similar scheme has been proposed for binary CSK in [7] for unbounded channels. In this case, each bit can be decoded sequentially via the detection rule

$$\tilde{s}_{n+1} = \begin{cases} 1 & R(n+1) > \tau, \\ 0 & \text{otherwise.} \end{cases} \tag{23}$$

The optimal choice of τ for the decision rule in (23) can then be obtained via an analysis of the probability of error. In particular,

$$P_e^{n,m,CSK}(\tau) \approx 0.5\left(1 - Q\left(\frac{\tau - M_p}{\sqrt{M_p + 2mM_e}}\right)\right) + 0.5Q\left(\frac{\tau}{\sqrt{2mM_e}}\right). \tag{24}$$

Assuming $2mM_e \gg M_p$, the variances of the both term are approximately the same and the corresponding threshold is given by

$\tau = M_p/2$. When each symbol is equally likely, $2mM_e = nM_e$. As such,

$$P_e^{n,m,CSK}(\tau) \approx 0.5\left(1 - Q\left(\frac{\tau - M_p}{\sqrt{M_p + nM_e}}\right)\right) + 0.5Q\left(\frac{\tau}{\sqrt{nM_e}}\right), \tag{25}$$

which is independent of m.

4.2 A Fair Choice of Parameters for Multi-Level Equilibrium Signaling

A desirable feature of the binary CSK scheme is that the sampling time t_{opt}^{CSK} is generally much shorter than the sampling time T_s for multi-level equilibrium signaling. As such, in order to provide a fair comparison, the number of levels M for multi-level equilibrium signaling should yield a data rate that is approximately the same.

In particular, let T_s be the required time for the system exploiting multi-level equilibrium signaling to approximately reach equilibrium. As detailed in [1], this time can be approximated (with small error ϵ corresponding to the gap to an equilibrium state) as,

$$T_s \approx \frac{L^2}{4D} - \frac{1}{a^1}\log\left(\frac{\epsilon}{\Delta}\right) - \frac{1}{a^2}\log\left(\frac{NV_{\text{vox}}}{NV_{\text{vox}} + 2V_{\text{Rx}}}\right). \tag{26}$$

In order to choose convenient number of levels M to provide a fair comparison with CSK, we require that

$$M = 2^{\left\lceil \frac{T_s}{t_{opt}^{CSK}} \right\rceil}. \tag{27}$$

Once the number of levels M is determined, the other issue is choosing transmission levels $\Delta^1, \Delta^2, \ldots, \Delta^M$. For the sake of a fair comparison with CSK, there should be an equal average number of molecules transmitted per bit. In conventional CSK, assuming equally likely transmission, the average number of transmission per bit is $\frac{\Delta}{2}$, Therefore, for multi-level equilibrium signaling, the number of molecules emitted for each symbol must satisfy

$$\frac{1}{M}\sum_{i=1}^{M}\Delta^i = \log_2 M\frac{\Delta}{2}. \tag{28}$$

To satisfy this constraint, we set $\Delta^1 = 0$ and impose equally spaced levels. That is, $\Delta^2 = \gamma$, $\Delta^3 = 2\gamma$ and $\Delta^M = (M-1)\gamma$, where γ is given by

$$\gamma = \frac{\Delta \log_2 M}{M-1}. \tag{29}$$

4.3 Sample Independence

In our development of multi-level equilibrium signaling, we have made the approximation (see, (11)) that multiple independent samples can be obtained for the quantity of S_1 in the receiver *for each symbol*. In order to verify that this assumption holds, we plot the autocorrelation function for $N_{\text{Tx},1}$ in Fig. 2(b) with the parameters presented in Section 4.4. Observe the rapid decay of the autocorrelation function, which implies near independence of samples given the statistics are approximately Gaussian.

Fig. 2(a) plots the autocorrelation function for $N_{\text{Tx},1}$ in the case of CSK with the same parameters. Observe that the decay of the magnitude of the autocorrelation function is significantly slower than for multi-level equilibrium signaling. This suggests that samples closely spaced in time are not independent, limiting the possibility of noise reduction via averaging.

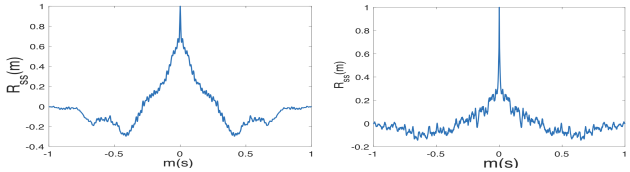

(a) Autocorrelation for $N_{\text{Tx},CSK}$ (CSK) (b) Autocorrelation for $N_{\text{Tx},1}$ (Equilibrium Signaling).

Figure 2: Autocorrelation functions of $N_{\text{Tx},1}$ and $N_{\text{Tx},CSK}$ for $a^1 = a^2 = 1\text{s}^{-1}$; $D_1 = D_2 = 1.51 \times 10^{-12}$ m^2/s, $\Delta = 500$, $V_{\text{Rx}} = V_{\text{Tx}} = \frac{L}{10}$, $L = 40 \times 10^{-5}$ and $x_d = 0.5L$.

4.4 Error Probability

We now turn to performance in terms of the probability of error. We assume that transmissions consist of $n = 160$ bits. For multi-level equilibrium signaling, gray coding is used to encode each symbol. Since the channel is non-stationary, the performance is evaluated in terms of the average number of errors in the sequence of n bits. More formally, let E_i be the error random variable for symbol i in the sequence; that is

$$E_i = \begin{cases} 1 & \hat{s}_i \neq s_i, \\ 0 & \hat{s}_i = s_i, \end{cases} \tag{30}$$

where $\hat{s}_i$ is the estimate of the transmitted bit s_i. Then, the average probability of error is defined as

$$P_{ave} = \mathbb{E}\left[\frac{1}{n}\sum_{i=1}^{n}E_i\right]. \tag{31}$$

In order to estimate P_{ave}, 10000 iterations of the transmission of n bits with different Δ are simulated. The parameters used in the simulations are: $a^1 = a^2 = 1\text{s}^{-1}$; $D_1 = D_2 = 1.51 \times 10^{-12}$ m^2/s and $V_{\text{Rx}} = V_{\text{Tx}} = \frac{L}{10}$ and $L = 40 \times 10^{-5}$ which are the same as in the microfluidic diffusion experiment setup in [10] and it is simulated via voxel-based approach as explained in detail in [8]. Unless stated, low memory detector is used to obtain corresponding BER curves.

In Fig. 3(d), the effect of number of samples on probability of error is plotted for different modulation levels M. Observe that increasing the number of samples per symbol dramatically reduces the probability of error. This is consistent with the fact that the samples are nearly independent. Moreover, since the number of molecules per bit is kept constant, 4-level equilibrium signaling has a lower probability of error than higher level signaling schemes as N_s increases. This is also expected since as M increases, the molecules used for each symbol decreases, which resulting in lower performance.

An illustrative performance comparison with CSK and multi-level equilibrium signaling is presented in Fig. 3(a) and Fig. 3(b). In these scenarios, the receiver is placed at $x = x_d$ while the transmitter is placed at $x = 0$. Using (27) for these setups, in Fig. 3(a), when

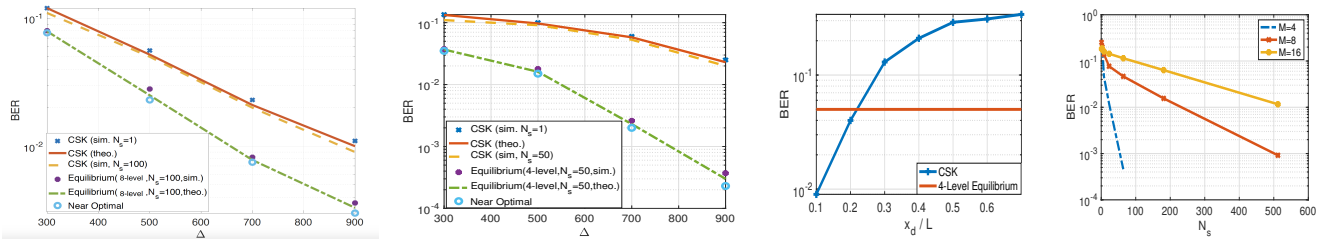

(a) BER performance comparison with CSK and $M = 8$ level equilibrium signaling for $x_d = 0.3L$.

(b) BER performance comparison with CSK and $M = 4$ for $x_d = 0.5L$.

(c) BER vs distance analysis for CSK and 4-Level Equilibrium for Δ=300 molecules and $N_s = 50$.

(d) BER vs number of samples for different multi-level equilibrium signaling with varying M and Δ=500 molecules.

Figure 3: BER performance of multi-level equilibrium signaling and CSK for different distances.

the receiver is closer to the transmitter $M = 8$ level is required to equalize data rate with CSK.

Observe in Fig.3(b) that when x_d increases (corresponding to an increase in the sampling time for CSK), $M = 4$ level equilibrium scheme is sufficient to equalize the data rate. As seen in Fig. 3(a) and Fig. 3(b), M-level equilibrium signaling outperforms CSK, even when both schemes use the same number, N_s, of samples per symbol. This is not surprising since in CSK, the observed samples are highly correlated with each other while in equilibrium signaling they are almost independent. As such, there is only a small improvement in the performance with CSK compared to that of equilibrium signaling, consistent with Fig. 3(d).

Another interesting property of equilibrium signaling is its robustness to geometric uncertainties and channel parameters such as distance. Since the observed signal statistics only depend on the transmitted signal and the volume of the channel, performance does not change as the distance x_d increases, which is not the case for CSK, illustrated in Fig. 3(c). Observe that the performance of CSK reduces as distance increases while for equilibrium signaling it is same for all distances x_d.

We also observe in Fig. 3(c) that for sufficiently large x_d, multi-level equilibrium signaling outperforms CSK. For small x_d, CSK leads to better performance since it has a greater mean peak value, M_p, for smaller distances. In these cases, the peak time t_{opt}^{CSK} is much smaller than equilibrium time T_s resulting in necessity of higher level equilibrium signaling which reduces the performance as observed in Fig. 3(d). However, the benefits of CSK are only obtained when the receiver has a good knowledge of the location of the transmitter and it is possible to properly optimize the sampling time.

5 CONCLUSION

In this paper, we addressed the problem of designing a molecular communication scheme that admits a detector that does not require full knowledge of the channel geometry and can support for higher order modulation schemes. We showed that our approach, called multi-level equilibrium signaling, can exploit multiple samples per symbol in order to reduce the probability of error. Moreover, multi-level equilibrium signaling admits a simple near optimal detection rule. We also show that our method can outperform conventional CSK schemes in a range of scenarios.

REFERENCES

[1] B. Akdeniz, M. Egan, and B.Q. Tang. 2020. Equilibrium signaling: molecular communication robust to geometry uncertainties. Preprint available https://hal.archives-ouvertes.fr/hal-02536318.

[2] Bayram Cevdet Akdeniz, Ali Emre Pusane, and Tuna Tugcu. 2018. Position-based modulation in molecular communications. *Nano communication networks* 16 (2018), 60–68.

[3] Hamidreza Arjmandi, Amin Gohari, Masoumeh Nasiri Kenari, and Farshid Bateni. 2013. Diffusion-based nanonetworking: A new modulation technique and performance analysis. *IEEE Communications Letters* 17, 4 (2013), 645–648.

[4] Hamidreza Arjmandi, Mohammad Zoofaghari, and Adam Noel. 2018. Diffusive Molecular Communication in a Biological Spherical Environment with Partially Absorbing Boundary. *arXiv preprint arXiv:1810.02657* (2018).

[5] Ge Chang, Lin Lin, and Hao Yan. 2017. Adaptive detection and ISI mitigation for mobile molecular communication. *IEEE Transactions on nanobioscience* 17, 1 (2017), 21–35.

[6] C.T. Chou. 2013. Extended master equation models for molecular communication networks. *IEEE Transactions on NanoBioscience* 12, 2 (2013), 79–92.

[7] Martin Damrath and Peter Adam Hoeher. 2016. Low-complexity adaptive threshold detection for molecular communication. *IEEE transactions on nanobioscience* 15, 3 (2016), 200–208.

[8] Johan Elf, Andreas Doncic, and Mans Ehrenberg. 2003. Mesoscopic reaction-diffusion in intracellular signaling. In *Fluctuations and noise in biological, biophysical, and biomedical systems*, Vol. 5110. International Society for Optics and Photonics, 114–125.

[9] S.N. Ethier and T.G. Kurtz. 2009. *Markov Processes: Characterization and Convergence*. John Wiley & Sons.

[10] Daniel Thomas Gillespie and Effrosyni Seitaridou. 2013. *Simple Brownian diffusion: an introduction to the standard theoretical models*. Oxford University Press.

[11] S.A. Isaacson. 2009. The reaction-diffusion master equation as an asymptotic approximation of diffusion to a small target. *SIAM J. Appl. Math.* 70, 1 (2009), 77–111.

[12] M.S. Kuran, H.B. Yilmaz, T. Tugcu, and I. Akyildiz. 2011. Modulation techniques for communication via diffusion in nanonetworks. In *IEEE International Conference on Communications (ICC)*.

[13] I. Llatser, A. Cabellos-Aparicio, M. Pierobon, and E. Alarcon. 2013. Detection techniques for diffusion-based molecular communnication. *IEEE Journal on Selected Areas in Communications* 31, 12 (2013), 726–734.